Redox Potentials of Active-Site Bis(cysteinyl) Fragments of Thiol-Protein Oxidoreductases†

Frank Siedler, Sabine Rudolph-Böhner, Masamitsu Doi,‡ Hans-Jürgen Musiol, and Luis Moroder*

Max Planck Institute of Biochemistry, 8033 Martinsried, Germany

Received February 18, 1993; Revised Manuscript Received April 13, 1993

ABSTRACT: The active sites of thiol-protein oxidoreductases consist of the characteristic Cys-X-X-Cys motif, and the redox potentials of these enzymes reflect the propensity of the bis(cysteinyl) sequence portion for disulfide loop formation. Thereby, as is known from comparing the three-dimensional (3D) structures of thioredoxin and glutaredoxin in the reduced and oxidized state, reduction of the disulfide bond is accompanied by minimal perturbation of the backbone folding of the active sites. In order to estimate the sequence-dependent intrinsic free energy of formation of the active-site disulfide loops in oxidoreductases, synthetic fragments corresponding to the sequences 31–38, 10–17, 134–141, and 34–41 of thioredoxin, glutaredoxin, thioredoxin reductase, and protein disulfide isomerase (PDI), respectively, were analyzed for their tendency to form 14-membered rings. For this purpose thiol/disulfide exchange experiments, with glutathione as reference redox pair, were performed on the bis(cysteinyl) octapeptides. As the free energy of ring closure of linear peptides consists mainly of the free energy of formation of the disulfide loop with a defined geometry from a statistical ensemble of conformations of the bis(cysteinyl) peptides, the observed differences in the equilibrium constants, although relatively small (within a factor 10), suggest that sequence-dependent information for loop formation is retained in the excised active-site fragments. These inherent redox potentials are, however, significantly affected and/or amplified in the native proteins by the conformational restraints imposed by the "structural domains" on the "functional domains".

The catalytic centers of thiol-protein oxidoreductases are contained within thiol/disulfide segments which exhibit the characteristic bis(cysteinyl) sequence motif Cys-X-X-Cys. Involvement of both cysteine residues in protein disulfide reduction has recently been unambiguously confirmed with mutants of *Escherichia coli* glutaredoxin (Bushweller et al., 1992). X-ray and ^{1}H-NMR three-dimensional (3D)[1] structures have been reported for several members of this superfamily of proteins. Correspondingly, structural data are available for *E. coli* thioredoxin in the reduced (Dyson et al., 1990) and oxidized forms (Holmgren et al., 1975; Katti et al., 1990), for reduced (Sodano et al., 1991) and oxidized (Xia et al., 1992) *E. coli* glutaredoxin, and for the oxidized phage T4 glutaredoxin (Söderberg et al., 1978; Eklund et al., 1992). In the known 3D structures the relatively small functional domains, i.e., the bis(cysteinyl) tetrapeptides, form hairpin-like loops which link a β-strand to an α-helix and which are partly surface-exposed within an accessible area of ca. 800 Å^2 (Xia et al., 1992). Despite the presence of this common bis(cysteinyl) sequence motif as active site, the biological properties of the various thiol-protein oxidoreductases are quite distinct, as substantiated by their remarkably differentiated redox potentials, which range from strongly reducing values, e.g., –0.27 V for thioredoxin (Krause et al., 1991), to greater oxidizing values, e.g., –0.11 V for the protein disulfide-isomerase (PDI) (Lyles & Gilbert, 1991; Hawkins et al., 1991).

Chain reversals in the active-site bis(cysteinyl) tetrapeptides Cys-X-X-Cys involve the effect of noncovalent interactions, and correspondingly of the tendency toward formation of turns, on the reactivity of the sulfhydryl and disulfide functions. In this context both the nature of the intervening sequence X-X and the conformational restraints imparted by the antiparallel folding of the N- and C-terminal peptide chain extensions should consistently affect the free energy of formation of the turn as well as of the disulfide bond. Therefore, a more or less favored disulfide bond formation defines the redox properties of the bis(cysteinyl)-based catalytic centers. Site-specific mutations have been performed in the active-site sequences of *E. coli* thioredoxin (Russel & Model, 1986; Gleason et al., 1990; Krause et al., 1991), bacteriophage T4 glutaredoxin (Joelson et al. 1990), and rat PDI (Lu et al. 1992) in the attempt to generate more PDI-like or thioredoxin-like enzymes, respectively. Although shifts of the redox potentials were induced by the mutations carried out in the intervening dipeptide sequence X-X, the conformational restraints imposed by the "structural domains" of the proteins on the "functional domains" seem to a large extent to dictate the redox properties despite the contiguous sequence character of the active sites.

In order to investigate this aspect more precisely and to determine the intrinsic redox properties of the catalytic centers of thiol-protein oxidoreductases when excised from their native protein structures, we have synthesized related fragments of *E. coli* thioredoxin and rat PDI, two enzymes well characterized in terms of their oxidation potential and protein disulfide isomerase activity, and of *E. coli* thioredoxin reductase and glutaredoxin as two additional representatives

† This research was supported by Grant Mo 377/3-1 of the Deutsche Forschungsgemeinschaft.

* Address correspondence to this author at the Max Planck Institute of Biochemistry, Am Klopferspitz 18a, D-8033 Martinsried, Germany.

‡ Research fellow of the Ministry of Education of Japan. Present address: Wakayama National College of Technology, Department of Industrial Chemistry, 77 Nashima, Nada-chou, Wakayama 644, Japan.

[1] Abbreviations: 3D, three-dimensional; PDI, protein disulfide isomerase; trx-His^{37}-[31–38], grx-[10–17], trr-[134–141], and PDI-[34–41], *N*-acetyl and *C*-amide derivatives of the active-site octapeptide sequences of thioredoxin, glutaredoxin, thioredoxin reductase, and PDI, respectively; DTT, dithiothreitol; GSH, reduced glutathione; GSSG, oxidized glutathione; EDTA, ethylenediaminetetraacetic acid; HPLC, high-performance liquid chromatography; TLC, thin-layer chromatography; RP, reversed-phase; t_R, retention time; R, reduced octapeptide; O, oxidized octapeptide; MD_1, MD_2, mixed disulfide (monoglutathione/peptide mixed disulfide); DD, double disulfide [bis(glutathione)/peptide mixed disulfide].

0006-2960/93/0432-7488$04.00/0

trx-His^{37}-[31-38] *Ac*-Trp-**Cys-Gly-Pro-Cys**-Lys-His-Ile-*NH*$_2$

grx-[10-17] *Ac*-Gly-**Cys-Pro-Tyr-Cys**-Val-Arg-Ala-*NH*$_2$

trr-[134-141] *Ac*-Ala-**Cys-Ala-Thr-Cys**-Asp-Gly-Phe-*NH*$_2$

PDI-[34-41] *Ac*-Trp-**Cys-Gly-His-Cys**-Lys-Ala-Leu-*NH*$_2$

FIGURE 1: Synthetic fragments corresponding to active-site sequences of thioredoxin (with Met^{37} replaced by a histidine residue), glutaredoxin, thioredoxin reductase, and PDI.

of this superfamily of proteins. Thereby were the active-site bis(cysteinyl) tetrapeptides extended N- and C-terminally in sequence mode to the octapeptides shown in Figure 1. This should allow conservative residues flanking the cysteines to exert their potential contributions to the loop formation. Furthermore, the excised fragments were capped as *N*-acetyl and *C*-amide derivatives in order to avoid possible end-group effects of the amino and carboxyl termini on the redox potentials, since studies on model bis(cysteinyl) peptides of varying intervening sequence length revealed that disulfide bond formation is affected by end groups (Zhang & Snyder, 1989). Moreover, the N- and C-terminally modified octapeptides should mimic more properly the catalytic sites in the native proteins. While in the case of glutaredoxin, thioredoxin reductase, and PDI native active-site sequences were synthesized, the methionine-37 residue of the thioredoxin active center would be expected to bring about significant difficulties in terms of the known facile oxidation of a thioether function to the corresponding sulfoxide in the various synthetic steps, particularly at the level of oxidative disulfide bond formation. It has therefore been replaced by a histidine in order to enhance the solubility and also in view of the high frequency of this residue in proximity to the cysteine pair, judged from a screening of 25 814 protein sequences according to the X-(His)-X(0–2)-Cys-X-X-Cys-X(0–2)-(His)-X motif. Besides leading to a surprisingly high number of matches (7237) for the Cys-X-X-Cys motif, the screening clearly revealed accumulation of histidine in the N-terminal (609) and C-terminal portions (701), respectively.

The synthetic active-site bis(cysteinyl) peptides were analyzed for their propensity to form cyclic monomers in thiol/disulfide exchange experiments using mixtures of oxidized (GSSG) and reduced glutathione (GSH) as redox buffer (Creighton, 1983). The apparent redox potentials of the bis(cysteinyl) peptides were estimated and compared with those of the native proteins in order to define the role of interactions in the folded state of the proteins in determining the redox properties of the "functional domains".

EXPERIMENTAL PROCEDURES

Materials

The N^{α}-acetyl octapeptide amides corresponding to active-site sequences 134–141 of *E. coli* thioredoxin reductase (trr-[134–141]), 10–17 of *E. coli* glutaredoxin (grx-[10–17]), 31–38 of *E. coli* thioredoxin with Met^{37} replaced by His (trx-His^{37}-[31–38]), and 34–41 of rat PDI (PDI-[34–41]) were prepared by conventional methods of synthesis in solution using an acid-labile side-chain protection in combination with the *S-tert*-butylthio group for the cysteine thiol functions. Upon deprotection of the octapeptide derivatives with trifluoroacetic acid in the presence of excess 2-methylindole as scavenger, RP chromatography at this intermediate state was carried out only for the trr-[134–141] peptide derivative, whereas similar intermediate purifications were prevented in the case of the other three peptide derivatives by their poor solubility. Final thiol deprotection was achieved by reduction of the unsymmetrical disulfides with tributylphosphine in aqueous trifluoroethanol (Moroder et al., 1981), and the resulting bis(cysteinyl) peptides were then oxidized in *N,N*-dimethylformamide at 10^{-3} M concentration with 0.5 equiv of azodicarboxylic acid di-*tert*-butyl ester (Mukaiyama & Takahashi, 1968). The resulting monomeric cyclic peptides were chromatographed on Fractogel TSK HW-40 S (Merck, Darmstadt, Germany) by elution with linear gradients of 2-propanol/1-butanol/NH_4OAc. The four cyclic octapeptide derivatives were carefully characterized in terms of their homogeneity and monomeric structure in order to reduce as much as possible experimental errors in the quantitation of products in thiol/disulfide exchange equilibria. (Details of the syntheses of the active-site octapeptide derivatives will be reported elsewhere.) The peptides were characterized as follows.

Ac-Ala-Cys-Ala-Thr-Cys-Asp-Gly-Phe-NH$_2$*(trr-[134–141]).* Quantitative amino acid analysis of the acid hydrolysate (6 M HCl containing 2.5% thioglycolic acid; 24 h at 110 °C): Asp, 1.00(1.0); Ala, 1.98(2.0); Thr, 0.83(1.0); Gly, 1.03(1.0); Cys, 1.77(2.0); Phe, 1.03(1.0); peptide content, 88.5% calcd for M_r = 825.28. The low recovery of Thr is known to be hydrolysis-dependent for Thr-Cys peptides (Wünsch et al., 1988). Gas chromatographic racemization test on Chirasil-Val glass capillary columns according to the method of Frank et al. (1977): D-Asp, 1.4%; D-Ala, 0.8%; D-Thr, 3.4%; D-Cys, n.d.; D-Phe, 0.4%. FABMS: m/z = 826; calcd M + H$^+$ = 826.29. The compound was homogeneous on TLC in different solvent systems and on HPLC (C-18, Nucleosil 300, Macherey-Nagel, Düren, Germany) with a linear gradient from CH_3CN/2% H_3PO_4 (13.2:86.8) to CH_3CN/2% H_3PO_4 (24.4:75.6). The extinction coefficient of 589 $M^{-1}cm^{-1}$ at 257.5 nm was determined on the basis of the peptide content (±3%) derived from quantitative amino acid analyses (three separate experiments).

Ac-Gly-Cys-Pro-Tyr-Cys-Val-Arg-Ala-NH$_2$*(grx-[10–17]).* Quantitative amino acid analysis of the acid hydrolysate (see above): Pro, 1.03(1.0); Gly, 0.98(1.0); Ala, 1.00(1.0); Cys, 1.90(2.0); Val, 0.96(1.0); Tyr, 1.00(1.0); Arg, 0.97(1.0); peptide content, 83.2% calcd for M_r = 906.38. Gas chromatographic racemization test: D-Pro, 1.0%; D-Ala, 0.5%; D-Val, 0.3%; D-Tyr, <0.3%; D-Arg, <0.5%. FABMS: m/z = 906; calcd M$^+$ = 906.38. The compound was homogeneous on TLC in different solvent systems and on HPLC (for conditions, see trr-[134–141]). The extinction coefficient of 1500 M^{-1} cm^{-1} at 276.5 nm was determined as described for trr-[134–141]).

Ac-Trp-Cys-Gly-Pro-Cys-Lys-His-Ile-NH$_2$*(trx-His*^{37}*-[31–38]).* Quantitative amino acid analysis of the acid hydrolysate (see above): Pro, 1.15(1.0); Gly, 1.00(1.0); Ile, 0.86(1.0); Cys, 1.78(2.0); His, 0.81(1.0); Lys, 0.97(1.0); Trp, 0.97(1.0); peptide content, 79.9% calcd for M_r = 981.43. Gas chromatographic racemization test: D-Pro, 1.3%; *allo*-Ile, 0.2%; D-Lys, 0.9%; D-His, <3%; D-Trp, n.d. FABMS: m/z = 982; calcd M + H$^+$ = 982.44. The compound was homogeneous on TLC in different solvent systems and on HPLC (for conditions, see trr-[134–141]). The extinction coefficient of 5600 M^{-1} cm^{-1} at 280.5 nm was determined as described for trr-[134–141].

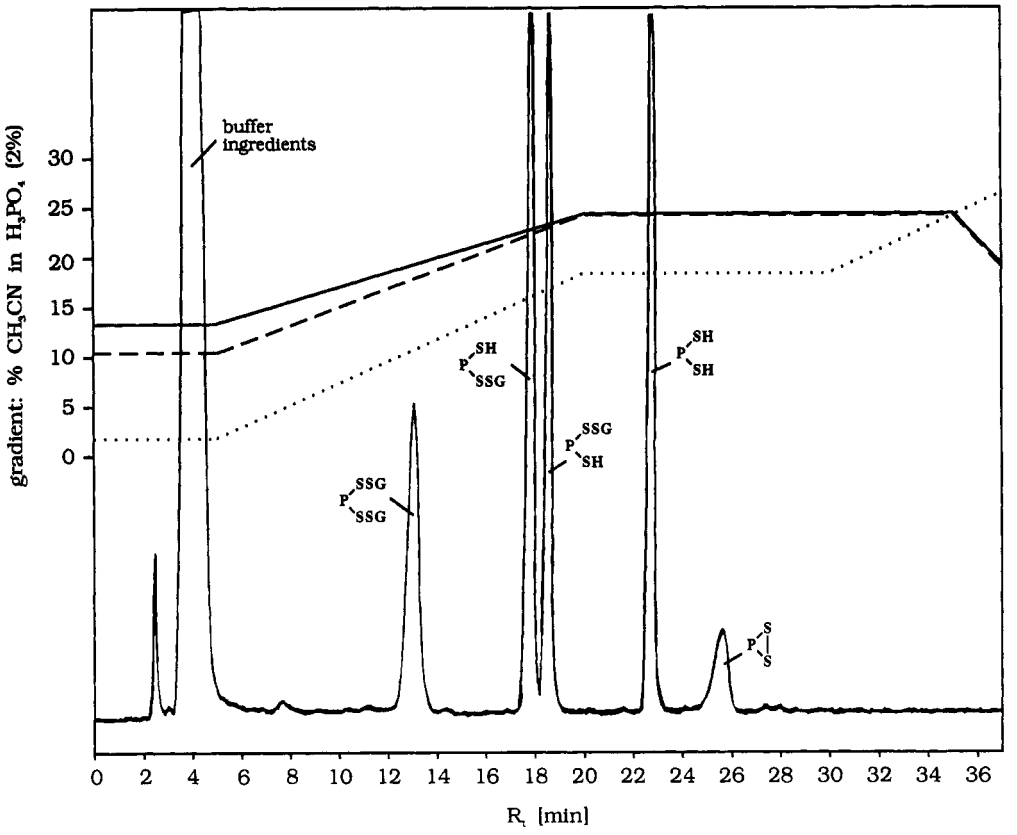

FIGURE 2: HPLC of an acid-quenched probe of the equilibrated thiol/disulfide exchange mixture of the thioredoxin peptide and GSH/GSSG (pH 7.0; T = 20.0 °C; [GSH] = 30 mM; [GSSG] = 10 mM). The optimized elution conditions are shown for the four peptides: trx-His^{37}-[31–38] and PDI-[34–41] (—); grx-[10–17] (- - -); trr-[134–141] (···).

Ac-Trp-Cys-Gly-His-Cys-Lys-Ala-Leu-NH$_2$(PDI-[34–41]). Quantitative amino acid analysis of the acid hydrolysate (see above): Ala, 1.01(1.0); Gly, 1.03(1.0); Leu, 1.00(1.0); Cys, 1.89(2.0); His, 0.99(1.0); Lys, 1.01(1.0); Trp, 0.97(1.0); peptide content, 83.1% calcd for M_r = 955.42. Gas chromatographic racemization test: D-Ala, <1%; D-Leu, 0.2%; D-Lys, 1.7%; D-His, <3%. FABMS: m/z = 956; calcd M + H$^+$ = 956.42. The compound was homogeneous on TLC in different solvent system and on HPLC (for elution conditions, see trr-[134–141]). The extinction coefficient of 5600 M^{-1} cm^{-1} at 280.5 nm was determined as described for trr-[134–141].

All reagents and solvents used in the present study were of the highest grade commercially available. GSH and GSSG (Sigma, Munich, Germany) were analyzed for purity by HPLC. GSSG contamination in GSH was found to be within the limits of error of the spectrophotometric assay with 2,2′-dithiopyridine (Grassetti & Murray, 1967). GSSG and GSH were used without further purification.

Thiol/Disulfide Exchange Equilibria

Equilibration. Equilibrations were carried out in plastic vials which were placed in a jacketed bath connected to a thermostat with temperature regulation of ±0.1 °C. Stock solutions were prepared by dissolving weighed samples of the cystine peptides and of GSH and GSSG in degassed and argon-flushed 0.1 M phosphate buffer containing 0.1 M NaCl and 1 mM EDTA (pH 7.0). Concentrations of the peptide samples were controlled by UV absorbance measurements, using the extinction coefficients reported above. Concentrations of GSSG were determined by weight and confirmed by UV measurements at 248 nm, using an extinction coefficient of 382 M^{-1} cm^{-1} (Chau & Nelson, 1991). Concentrations of GSH were determined spectrophotometrically with 2,2′-dithiopyridine (Grassetti & Murray, 1967). After the components were mixed at the various ratios, the solutions (2 mL) were gently flushed with argon prior to incubation in the thermostated bath.

Quenching. In order to assess possible perturbations of the equilibria by the quenching method, acid quenching with different amounts of phosphoric acid or irreversible derivatization with excess *N*-ethylmaleimide was performed. While the latter method was found to be inappropriate, particularly regarding the HPLC pattern, the acid quenching procedure (Lin & Kim, 1989; Zhang & Snyder, 1989) allowed us to obtain reproducible data. It was therefore used routinely as follows: 100-μL samples of the reaction mixtures were taken under a soft argon stream and injected into 40 μL of 1 M phosphoric acid to lower immediately the pH to a value of 2.0; the samples were quickly vortexed under argon, frozen, and stored at −18 °C until used for HPLC analyses, which were performed within 12 h.

Chromatographic Separation and Quantitation of the Reaction Products. All equilibration mixtures were analyzed by HPLC on a C-18 Nucleosil 300 column (4 mm × 300 mm, 5 μm; Macherey-Nagel, Düren, Germany) using binary linear gradients of CH$_3$CN/2% H$_3$PO$_4$ as eluents at a flow rate of 0.8 mL/min; UV absorbance was monitored at 210 nm. The gradient composition was optimized for each experiment to achieve base-line separation of all components of the thiol/disulfide exchange equilibria. A typical chromatogram is shown in Figure 2 for the thioredoxin peptide; the elution conditions for all four peptides are also reported in Figure 2. The retention times (t_R) of the reaction components, i.e., of GSSG, GSH, cyclic monomers, and fully reduced octapeptides, were determined with authentic samples. Regarding the mixed

disulfides, a preparative-scale experiment was performed with the glutaredoxin peptide. After equilibration, RP chromatography on LiChroprep RP 18 (Merck, Darmstadt, Germany) [eluents: 98% 0.1 M NH_4OAc/2% 2-propanol (buffer A) and 88% 0.1 M NH_4OAc/10% 2-propanol/2% 1-butanol (buffer B); 5-h isocratic elution with A, 12-h elution with a linear gradient from A to B; column, 0.63 cm × 100 cm; flow rate, 30 mL/h] allowed us to isolate, besides the cyclic monomeric grx-[10–17], the bis(glutathione)/peptide mixed disulfide and to identify the latter unambiguously by quantitative amino acid analysis. The monoglutathione/peptide mixed disulfides could not be isolated by this procedure because of their instability (conversion to the cyclic monomer). The HPLC peak with the lowest t_R among the unassigned ones was found to correspond to bis(glutathione)/grx-[10–17], determined by comparison with the authentic sample. Two additional peaks remained unassigned. The intermediate t_R values of these two components together with the observed instability of the substances corresponding to these two peaks (see above) induced us to assign them to the monoglutathione/peptide mixed disulfides. This is further supported by the observation that this pair of peaks, although changing in intensity as a function of the [GSH]/[GSSG] ratio, exhibits similar intensities for the two components as expected for the two possible monoglutathione adducts. Taking into account the strong similarity between the elution patterns of the four peptides, peaks of the HPLC chromatograms of trr-[134–141], trx-His^{37}-[31–38], and PDI-[34–41] were assigned by analogy.

Assuming quantitative elution of the reaction components from the HPLC columns, concentrations of the reduced and oxidized species at equilibrium were correlated to the peak areas as follows: The reduced and oxidized peptide species exhibit identical extinction coefficientes at 210 nm, within the limits of error of the spectroscopic measurements, confirmed in separate experiments by measuring UV spectra of the oxidized peptides and, upon quantitative reduction with DTT, of the reduced species. The extinction coefficients of the monoglutathione/peptide and bis(glutathione)/peptide mixed disulfides were computed from the components. The close agreement of the calculated and experimental values determined for the isolated bis(glutathione) adduct in the case of the glutaredoxin peptide confirmed the validity of this procedure. This was further supported by the total balance of peptide species (±3%) in the single series of experiments.

Equilibrium Constants. The oxidized octapeptide derivatives (0.143 mM in the above mentioned buffer) were exposed to the thiol/disulfide exchange reaction in the presence of a large excess of glutathione (50 mM) at six different [GSH]/[GSSG] ratios (trx-His^{37}-[31–38], 0.63, 0.94, 1.33, 2.00, 3.00, and 4.8; trr-[134–141], 1.30, 2.06, 3.07, 4.79, 8.46, and 18.30; grx-[10–17], 1.30, 2.00, 3.00, 4.67, 8.00, and 18.30; PDI-[34–41], 0.90, 1.33, 2.00, 4.67, and 8.00). Establishment of equilibria in the samples (2-mL final volume) incubated at 10, 20, and 37 °C was assessed by analyzing 100-μL quenched samples at increasing time intervals by HPLC until the pattern of distribution of the single components was found to be stable. Spectrophotometric determination of total thiol content with 2,2′-dithiopyridine (Grassetti & Murray, 1967) indicated that there was no significant loss of thiol groups (<1%) caused by any residual oxygen in the reaction vessels.

Data Analysis. In the network of equilibria given in Figure 3, the single steps can be considered as separate entities according to the "principle of detailed balancing" (Weston et al., 1972). Fractional values defined with respect to the more reduced species, R_{xy}, lead to eqs 1–9.

$$R_{11} = \frac{[R]}{[R] + [MD_1]} = \frac{\frac{[GSH]}{[GSSG]}}{K_{11} + \frac{[GSH]}{[GSSG]}} \quad (1)$$

$$R_{12} = \frac{[MD_1]}{[O] + [MD_1]} = \frac{[GSH]}{K_{12} + [GSH]} \quad (2)$$

$$R_{13} = \frac{[MD_1]}{[DD] + [MD_1]} = \frac{\frac{[GSH]}{[GSSG]}}{K_{13} + \frac{[GSH]}{[GSSG]}} \quad (3)$$

$$R_{21} = \frac{[R]}{[R] + [MD_2]} = \frac{\frac{[GSH]}{[GSSG]}}{K_{21} + \frac{[GSH]}{[GSSG]}} \quad (4)$$

$$R_{22} = \frac{[MD_2]}{[O] + [MD_2]} = \frac{[GSH]}{K_{22} + [GSH]} \quad (5)$$

$$R_{23} = \frac{[MD_2]}{[DD] + [MD_2]} = \frac{\frac{[GSH]}{[GSSG]}}{K_{23} + \frac{[GSH]}{[GSSG]}} \quad (6)$$

$$R_{ox} = \frac{[R]}{[R] + [O]} = \frac{\frac{[GSH]^2}{[GSSG]}}{K_{ox} + \frac{[GSH]^2}{[GSSG]}} \quad (7)$$

$$R_{DD} = \frac{[R]}{[R] + [DD]} = \frac{\frac{[GSH]^2}{[GSSG]^2}}{K_{DD} + \frac{[GSH]^2}{[GSSG]^2}} \quad (8)$$

$$R_{ret} = \frac{[O]}{[O] + [DD]} = \frac{\frac{1}{[GSSG]}}{K_{ret} + \frac{1}{[GSSG]}} \quad (9)$$

The single equilibrium constants, defined as

$$K_{11} = \frac{[MD_1][GSH]}{[R][GSSG]} \qquad K_{21} = \frac{[MD_2][GSH]}{[R][GSSG]}$$

$$K_{12} = \frac{[O][GSH]}{[MD_1]} \qquad K_{22} = \frac{[O][GSH]}{[MD_2]}$$

$$K_{13} = \frac{[DD][GSH]}{[MD_1][GSSG]} \qquad K_{23} = \frac{[DD][GSH]}{[MD_2][GSSG]}$$

$$K_{ox} = \frac{[O][GSH]^2}{[R][GSSG]} \qquad K_{DD} = \frac{[DD][GSH]^2}{[R][GSSG]^2}$$

$$K_{ret} = \frac{[DD]}{[O][GSSG]}$$

were estimated from the rectangular hyperbolic correlation curves by nonlinear regression calculations using the program package GraFit 2.0 (Leatherbarrow 1990). Similarly, the

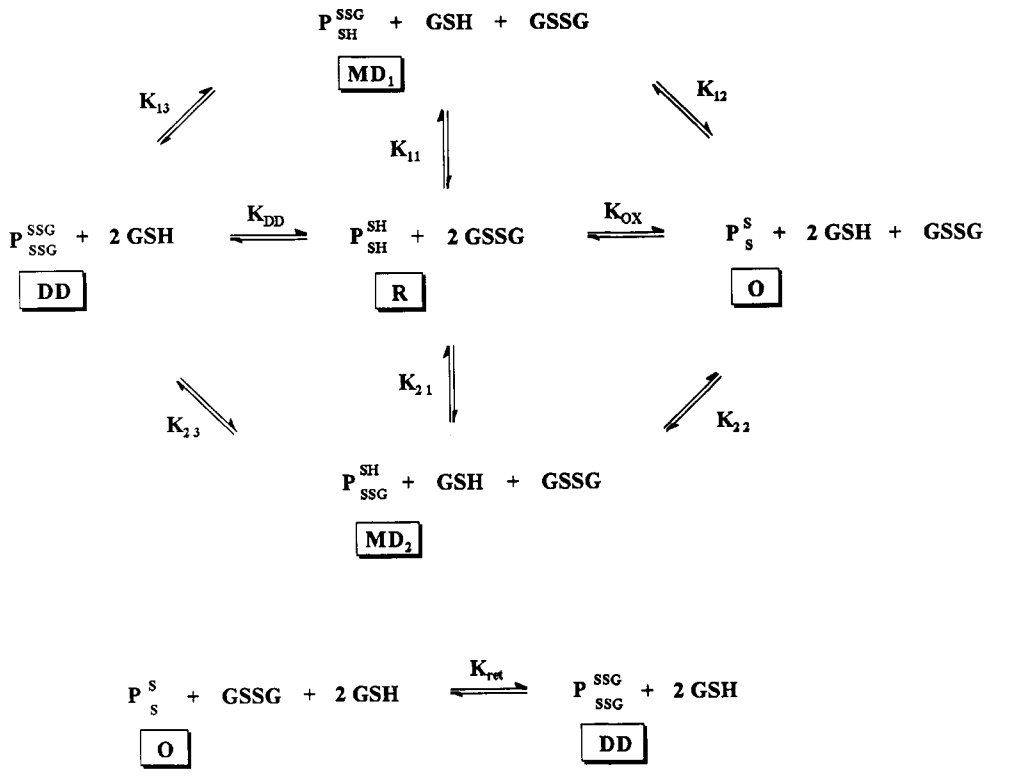

FIGURE 3: Thiol/disulfide exchange reactions of bis(cysteinyl) peptides in glutathione redox buffer: P^{SH}_{SH}, reduced peptide; P^{S}_{S}, cyclic monomer; P^{SSG}_{SH}, monoglutathione/peptide mixed disulfide; P^{SSG}_{SSG}, bis(glutathione)/peptide mixed disulfide.

overall equilibrium constants K_{ox}, K_{DD}, and K_{ret} were estimated from the correlation curves as well as computed for comparison using eqs 10–12.

$$K_{ox} = K_{11}K_{12} = K_{21}K_{22} \quad (10)$$

$$K_{DD} = K_{11}K_{13} = K_{21}K_{23} \quad (11)$$

$$K_{ret} = \frac{K_{DD}}{K_{ox}} = \frac{K_{13}}{K_{12}} = \frac{K_{23}}{K_{22}} \quad (12)$$

$$E_0 = E_0(\text{glutathione}) - 0.03 \log K_{ox} \quad (13)$$

The apparent redox potentials of the bis(cysteinyl) peptides were calculated according to eq 13 using a redox potential, E_0, for glutathione of –0.24 V (Rost & Rapoport, 1964). Van't Hoff plots of ln K_{ox} *vs* $1/T$ allowed us to extrapolate the values of the thermodynamic parameters ΔH, ΔS, and ΔG.

RESULTS

The complex network of reactions taking place in the thiol/disulfide exchange reaction of the bis(cysteinyl) peptides in the GSH/GSSG redox buffer is shown in Figure 3. Besides the two glutathione components, the reduced and oxidized peptide species, the two monoglutathione/peptide mixed disulfides, and the bis(glutathione)/peptide mixed disulfide, even oligomers, i.e., dimers and polymers, could be formed in this reaction. However, HPLC analysis of the reaction mixtures at equilibrium did not reveal formation of oligomers to any clearly detectable extent under the different chromatographic conditions examined. As shown representatively in Figure 2 for the equilibrated thiol/disulfide exchange mixture of trx-His^{37}-[31–38], under optimized conditions the single peaks of the HPLC chromatograms were base-line separated, thus allowing quantitative analysis of the single components with minimal errors. Moreover, the system is sufficiently well defined at equilibrium to determine the equilibrium constants of the single reaction steps according to the procedure described under Data Analysis.

Equilibration was performed for each peptide at 10, 20, and 37 °C with GSH/GSSG at six different ratios, whereby the total glutathione concentration ([GSH] + 2[GSSG]) of 50 mM was kept constant and much greater than the peptide concentration (0.143 mM). By this procedure the glutathione redox pair dictates the redox potential of the system. Incubation of the peptides with GSH/GSSG at different ratios leads to different fractions of the more reduced species at equilibrium according to eqs 1–9. Plots of the fractional values of the concentration of the more reduced species *vs* [GSH]/[GSSG] (eqs 1, 3, 4, and 6), [GSH] (eqs 2 and 5), $[GSH]^2/[GSSG]$ (eq 7), $[GSH]^2/[GSSG]^2$ (eq 8), and $[GSSG]^{-1}$ (eq 9) allowed us to determine the K values through nonlinear regressions (Table I). The equilibrium constants obtained by this procedure were in excellent agreement with the average K values deduced from the experimental data, thus confirming the validity of our model. This is further supported by the observation that the K_{ox}, K_{DD}, and K_{ret} values determined directly from the rectangular hyperbolas coincide within the limits of error of ±5% with the K values calculated according to both thermodynamic linkages given in eqs 10, 11, and 12, respectively.

The overall K_{ox} values of the four peptides were found to differ among themselves only within a factor of 10 in sequence dependency as follows: trx-His^{37}-[31–38] < PDI-[34–41] < trr-[134–141] < grx-[10–17]. This rank order of the excised active-site fragments is opposite that of the apparent redox potentials of the oxidoreductases, except for PDI (see Table II).

Regarding the equilibrium constants of the single steps, it seems worthwhile noting that in the case of PDI-[34–41] and trx-His^{37}-[31–38] formation of one of the two possible mono mixed disulfides is apparently preferred to the other. A reasonable explanation for this observation could be the

Table I: Equilibrium Constants (K Values) of the Single Reaction Steps of Thiol/Disulfide Exchange Experiments Using the GSH/GSSG System as Redox Buffer[a]

substance	temp [°C]	K_{11}	K_{21}	K_{12} [M]	K_{22} [M]	K_{13}	K_{23}	K_{DD}	K_{ret} [M]$^{-1}$	K_{ox} [M]
trx-His^{37}-[31–38]	10	2.71	2.05	0.0056	0.0074	1.80	2.37	4.87	320.57	0.015
	20	2.43	1.89	0.0066	0.0084	1.71	2.18	4.14	259.93	0.016
	37	2.55	2.08	0.0105	0.0128	1.86	2.28	4.74	177.40	0.027
trr-[134–141]	10	1.86	1.87	0.0609	0.0610	1.59	1.57	2.95	25.93	0.114
	20	1.88	1.87	0.0652	0.0660	1.52	1.54	2.87	23.32	0.123
	37	1.99	2.06	0.0763	0.0740	1.56	1.50	3.10	20.36	0.152
grx-[10–17]	10	2.68	2.57	0.0427	0.0441	2.27	2.37	6.09	53.44	0.114
	20	2.67	2.61	0.0533	0.0545	2.25	2.31	6.02	42.31	0.142
	37	2.69	2.72	0.0710	0.0702	2.25	2.22	6.05	31.68	0.191
PDI-[34–41]	10	2.65	2.07	0.248	0.0314	1.97	2.50	5.20	79.55	0.065
	20	2.64	2.11	0.0300	0.0374	2.04	2.54	5.38	67.89	0.079
	37	2.59	2.12	0.0393	0.0477	1.98	2.41	5.12	50.47	0.101

[a] Error of all values ≤5%. If not stated otherwise, K values are without dimensions.

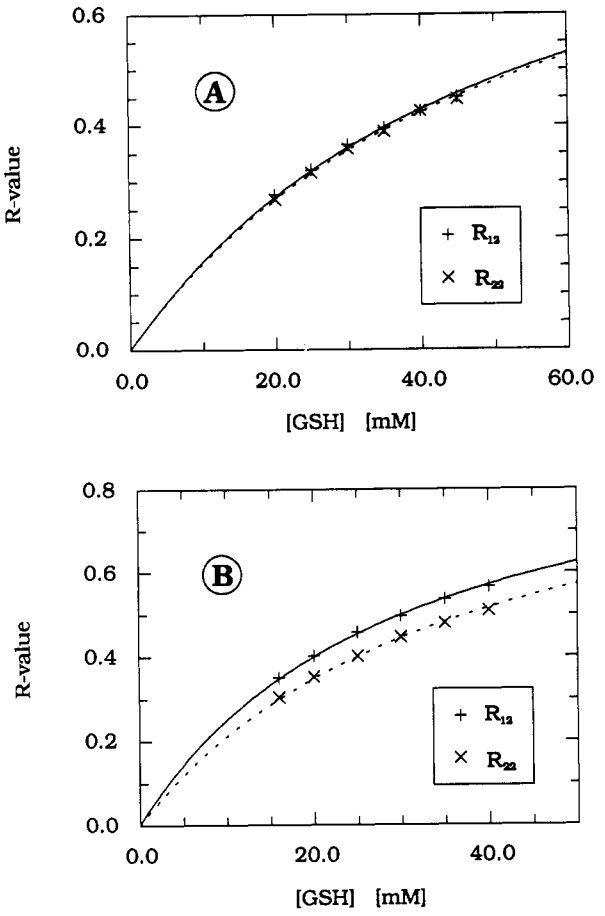

FIGURE 4: Nonlinear regression plots of R_{12} and R_{22} vs [GSH] in the case of grx-[10–17] (A) and PDI-[34–41] (B) (pH 7.0; T = 20.0 °C).

presence of a histidine residue in the vicinity of the second cysteine residue of the Cys-X-X-Cys motif in these two peptides. This fact could facilitate the nucleophilic attack by this cysteine thiolate species on the GSSG disulfide group. A similar effect could potentially be exerted by the lysine residue located adjacent to the second cysteine in the PDI and thioredoxin peptides. However, in the glutaredoxin peptide an arginine is in the vicinity of the second cysteine, but without a similar effect. Moreover, as mentioned above, we were unable to isolate the monoglutathione mixed disulfides in order to assign their structures and, thus, to validate this hypothetical explanation for the observed different reactivities of the two cysteines in the thioredoxin and PDI peptides.

The equilibrium constants K_{12} and K_{22} related to the intramolecular cyclization of the mixed disulfides are in the order of magnitude of those determined for model Cys-X-X-Cys peptides (Zhang & Snyder, 1989). But surprisingly the rank order determined for this reaction step, i.e., trr-[134–141] > grx-[10–17] > PDI-[34–41] > trx-His^{37}-[31–38] was found to be identical to that of the redox potentials of the enzymes, except for thioredoxin.

Table II: Apparent Redox Potentials of the Active-Site Fragments at 20 °C[a]

substance	E_0 [mV] enzyme	E_0 [mV] fragment
thioredoxin	−270[b]	−190
thioredoxin reductase	−250[c]	−210
glutaredoxin	ca. −230[d]	−215
PDI	−110[e]	−205

[a] For comparison, the redox potentials of the parent enzymes are reported. [b] At pH 7.0 (Krause et al., 1991). [c] At pH 7.0 (O'Donnell & Williams, 1983). [d] The redox potential of T4 glutaredoxin is −230 mV (Nilsson et al., 1990); the redox potential of glutaredoxin should be in the same range. [e] At pH 7.5 (Hawkins et al., 1991).

Employing glutathione as reference thiol, formation of whose corresponding disulfide bond does not depend on urea (Creighton, 1977) and is thus free from conformational constraints, and assuming that the inherent free energy of formation of the disulfide bond in GSSG and in the bis(cysteinyl) peptides is identical, the K_{ox} values as "effective concentrations" (C_{eff}) (Creighton, 1983, 1986) should provide information about the probability that the two cysteine thiols in the peptides are correctly positioned to form a disulfide bond. In this context it is interesting that the C_{eff} value of the thioredoxin peptide of 20 mM compares well with the C_{eff} of 26 mM determined for thioredoxin in the denaturated state, i.e., in the absence of structural effects of the folded protein (Lin & Kim, 1989). This value also agrees with the observation of Zhang and Snyder (1989) that formation of a disulfide bond in unstructured peptides is associated with C_{eff} values in the range of tens of millimolar. Similarly, reoxidation experiments on apamin have shown that the effective concentration of forming the first disulfide from unstructured apamin is approximately 25 mM, whereas the C_{eff} for the second disulfide is 17 M, resulting from the high cooperativity of the refolding process (Huyghues-Despointes & Nelson, 1992). The higher K_{ox} values determined for the glutaredoxin, thioredoxin reductase, and PDI peptides (Table I) should therefore indicate a higher conformational preference for ring closure. This seems to be supported by the circular dichroism of the bis(cysteinyl) peptides in aqueous solution, which, although dominated by random-coil contributions and the difficulty of unambiguous interpretation because of the strong aromatic contributions, suggests the presence of ordered

Table III: Thermodynamic Parameters Determined from the Temperature Dependency of the K_{ox} Values[a]

substance	$\Delta G°$ (kJ mol^{-1})	$\Delta H°$ (kJ mol^{-1})	$\Delta S°$ (J K^{-1} mol^{-1})
trx-His^{37}-[31–38]	9.6		
trr-[134–141]	5.1	7.9	9.8
grx-[10–17]	4.8	13.9	31.1
PDI-[34–41]	6.2	11.8	19.0

[a] The $\Delta G°$ values calculated directly from the K_{ox} values were found to be identical with those determined from the van't Hoff plots.

structure to some extent in grx-[10–17], PDI-[34–41], and trr-[134–141] but not in trx-His^{37}-[31–38] (unpublished results).

The effect of temperature on the overall K_{ox} of each of the four peptides was found to be weak but was detectable at least for the PDI, thioredoxin reductase, and glutaredoxin peptides. Among the various reactions involved in the thiol/disulfide exchange, formation of the monoglutathione mixed disulfides and the cyclization process were particularly temperature-dependent. This temperature dependency is also mirrored in the overall K_{ox} values. The good correlations in the van't Hoff plots (R_{trr} = 0.989; R_{grx} = 0.999; R_{PDI} = 0.998) allowed us to determine the thermodynamic parameters (Table III), which, however, have to be considered only as indicative values because of the limited number of temperature-dependent experiments. Sandberg et al. (1991) have determined the free energy associated with the disulfide loop formation and, thus, with the stabilization of thioredoxin (–13.4 kJ/mol) and glutaredoxin (3.8 kJ/mol) in the oxidized state. The $\Delta G°$ of 4.8 kJ/mol determined for the disulfide loop formation of the glutaredoxin active-site fragment compares well with the $\Delta G°$ related to this ring closure in the intact protein, a fact which fully agrees with the similar redox potentials of the protein and the protein fragment (Table II). In contrast, a striking difference in the $\Delta G°$ values is observed in the case of thioredoxin, where in the native protein the conformational restraints imparted by the 3D structure in the reduced state apparently favor the formation of the 14-membered ring in a decisive manner. Furthermore, a comparison of the entropic contributions suggests a weaker impact of the unfavored 14-membered ring size on the configurational entropy in the case of the glutaredoxin peptide than in the case of the thioredoxin reductase and PDI peptides.

DISCUSSION

The 3D structure of the active-site portion Cys-Gly-Pro-Cys of thioredoxin, in both the reduced and the oxidized state, exhibits a chain reversal with Cys^1 located in position i + 3 of a type I β-turn and Pro^3 at the beginning of a long α-helical stretch with a transannular hydrogen bond between Cys^1 and Cys^4. Similarly, reduction of glutaredoxin provokes only minimal perturbations of the peptide backbone conformation. Circular dichroism and ^{1}H-NMR conformational studies have been performed previously on the cyclic tetrapeptide derivatives Boc-Cys-Gly-Pro-Cys-NHMe and Boc-Cys-Pro-Tyr-Cys-NHMe of the thioredoxin and glutaredoxin active sites, respectively (Ravi & Balaram, 1983; Kishore et al. 1988). For the thioredoxin model peptide a conformation in aprotic solvents has been proposed which consists of two consecutive type III β-turns (incipient 3_{10} helix) with Gly-Pro and Pro-Cys as the corner residues stabilized by two intramolecular 4 → 1 hydrogen bonds involving Cys^{1}CO → NHCys^4 and Gly^{2}CO → NHMe. This structure is strongly reminiscent of the thioredoxin active site, whereas the structure proposed for the glutaredoxin model peptide, i.e., a type I β-turn, would be different from the active-site 3D structure of this protein. As these results obtained in aprotic solvents do not answer in a satisfactory manner the question of whether the excised fragments in aqueous solution exhibit chain reversals identical to or different from those of the native proteins, we have estimated to a first approximation the propensities for chain reversals from the frequencies of occurrence of amino acids in β-turns (Chou & Fasman, 1977). A rank order of β-turn probabilities of grx-[10–17] (6.5×10^{-4}) ≫ PDI-[34–41] (1.5×10^{-4}) > trr-[134–141] (9.4×10^{-5}) > trx-His^{37}-[31–38] (5.5×10^{-5}) was obtained for the Cys-X-X-Cys sequences whereby all values, except for that of thioredoxin, were above the average β-bend potential of 5.5×10^{-5}. In thiol/disulfide exchange experiments which should allow the formation of thermodynamically favored structures at equilibrium, the K_{ox} values related to the formation of the cyclic monomers were in the order grx-[10–17] > trr-[134–141] > PDI-[34–41] > trx-His^{37}-[31–38] (Table I), which is not fully in line with the computed β-turn potentials of the peptides. In model studies where β-turns were similarly stabilized by disulfide bonds, good agreement with β-turn potentials was reported (Venkatachalapathi et al., 1982; Ravi & Balaram, 1983, 1984; Milburn et al., 1987, 1988; Kishore et al. 1988; Falcomer et al., 1992). In the present study the Cys-X-X-Cys sequence is N-terminally and, particularly, C-terminally extended. The free energy of formation of a disulfide loop consists not only of the free energy of formation of a turn from a statistical ensemble of conformations in the dipeptide portion X-X but also of the free energy of formation of an extended conformation in the two cysteine residues, which leads to a hairpin-like antiparallel β-sheet and which involves interactions between these two residues (Falcomer et al., 1992). Therefore, exocyclic adjacent residues can affect the product distribution in thiol/disulfide exchange equilibria. This seems to be the case with the octapeptides examined in the present study; it is further supported by our previous observation on the octapeptide fragment 225–232 of the human IgG1 hinge region, i.e., H-Thr-Cys-Pro-Pro-Cys-Pro-Ala-Pro-OH with Pro-Pro as the intervening sequence of the Cys-X-X-Cys motif. Although even for this peptide a high propensity for chain reversal with a $\langle p_t \rangle = 1.9 \times 10^{-4}$ was predicted, air oxidation performed under conditions which allowed thiol/disulfide exchange to take place led to almost exclusive formation of the dimer in parallel alignment, as is present in the native protein (Moroder et al., 1990). Since the 3D structure of this IgG1 fragment was found to be practically identical to that in the native Kol protein (Kessler et al. 1991), it behaved like a protein subdomain.

Conversely, the active-site fragments of the oxidoreductases examined in this study do not seem to exhibit a similarly strong protein subdomain character. In fact, the K_{ox} values of the excised fragments of glutaredoxin and thioredoxin reductase were about 10 times lower, and in the case of thioredoxin about 100 times lower, than those of the native proteins. In contrast, the PDI peptide was found to exhibit a K_{ox} value which is 2000 times higher than that of the enzyme. This fact is reflected by the apparent redox potentials, which differ significantly from those of the native proteins except for glutaredoxin, shown in Table II. Thioredoxin [E_0 = –0.270 V (Krause et al., 1991) or –0.265 V (Salamon et al., 1992)] is known to be more reducing than thioredoxin reductase [E_0 = –0.254 V (O'Donnell & Williams, 1983)] and significantly more reducing than PDI [E_0 = –0.11 (Lyles & Gilbert, 1991;

Hawkins et al., 1991)]. Regarding glutaredoxin, to our knowledge the redox potential has not yet been determined, but it should be in the range of that of T4 glutaredoxin [E_0 = –0.23 V (Nilsson et al., 1990)]. On the other hand, the redox potentials of the peptides differ only slightly among themselves; the strongest deviations from the values of the native enzymes were obtained for PDI-[143–141] and trx-His^{37}-[31–38]. This raises the question of whether substitution of Met^{37} in the trx sequence with histidine is responsible for the more PDI-peptide-like redox properties of trx-His^{37}-[31–38], a fact which would agree with the observed higher reactivity of one cysteine residue possibly resulting from the proximity of a histidine in both peptides.

The results of the present study confirm that the redox potentials of the thiol-protein oxidoreductases are largely dictated by the juxtaposition of the cysteine residues resulting from interactions in the folded state of the proteins. From data available so far for thioredoxin and glutaredoxin it can be assumed that in the intact proteins the backbone folding of the active site is practically identical in the reduced and oxidized states. Therefore, the free energy of the formation of the 14-membered ring is mainly dictated by the geometry imposed on the Cys-X-X-Cys motif by the 3D structure of the proteins, whereby the entropic contribution would mainly be associated with the array of the cysteine side chains. This is supported by the observation that mutations performed in the active site of thioredoxin, T4 glutaredoxin, and PDI were found to induce remarkably stronger changes of the redox potentials than those observed in the octapeptides. Thus, the sequence-intrinsic free energy for the formation of the 14-membered ring is strongly affected and/or amplified by the conformational restraints of the protein structure. This effect is particularly evident for PDI and thioredoxin; disulfide loop formation is hindered by a factor 2000 in the case of PDI and favored by a factor 100 in the case of thioredoxin when compared with the excised fragments.

ACKNOWLEDGMENT

The authors are grateful to Mrs. Sheila A. Daniels for carefully reading the manuscript and to Dr. A. Ogrodnik (TU München) for helpful discussions.

REFERENCES

Bushweller, J. H., Åslund, F., Wüthrich, K., & Holmgren, A. (1992) *Biochemistry 31*, 9288–9293.
Chau, M.-H., & Nelson, J. W. (1991) *FEBS Lett. 291*, 296–298.
Chou, P. Y., & Fasman, G. D. (1977) *J. Mol. Biol. 115*, 135–175.
Creighton, T. E. (1983) *Biopolymers 22*, 49–56.
Creighton, T. E. (1986) *Methods Enzymol. 131*, 83–106.
Dyson, H. J., Gippert, G. P., Case, D. A., Holmgren, A., & Wright, P. E. (1990) *Biochemistry 29*, 4129–4136.
Eklund, H., Sonnerstam, U., Ingelman, M., Söderberg, B.-O., Uhlin, T., Nordlund, P., Nikkola, M., Joelsson, T., & Petratos, K. (1992) *J. Mol. Biol. 228*, 596–618.
Falcomer, C. M., Meinwald, Y. C., Choudhary, I., Talluri, S., Milburn, P. J., Clardy, J., and Scheraga, H. A. (1992) *J. Am. Chem. Soc. 114*, 4036–4032.
Frank, H., Nicholson, G. I., & Bayer, E. (1977) *J. Chromatogr. Sci. 15*, 174–176.
Gleason, F. K., Lim, C.-J., Gerami-Nejad, M., & Fuchs, J. A. (1990) *Biochemistry 29*, 3701–3709.
Grassetti, D. R., & Murray, J. F., Jr. (1967) *Arch. Biochem. Biophys. 119*, 41–49.
Hawkins, H. C., de Nardi, M., & Freedman, R. B. (1991) *Biochem. J. 275*, 341–348.
Holmgreen, A., Söderberg, B.-O., Eklund, H., & Brändén, C. I. (1975) *Proc. Natl. Acad. Sci. U.S.A. 72*, 2305–2309.
Huyghues-Despointes, B. M. P., & Nelson, J. W. (1992) *Biochemistry 31*, 1476–1483.
Joelson, T., Sjöberg, B.-M., & Eklund, K. (1990) *J. Biol. Chem. 265*, 3183–3188.
Katti, S. K., LeMaster, D. M., & Eklund, H. (1990) *J. Mol. Biol. 212*, 167–184.
Kessler, H., Mronga, S., Müller, G., Moroder, L., & Huber, R. (1991) *Biopolymers 31*, 1189–1204.
Kishore, R., Raghothama, S., & Balaram, P. (1988) *Biochemistry 27*, 2462–2471.
Krause, G., Lunström, J., Barea, J. L., Pueyo de la Cuesta, C., & Holmgren, A. (1991) *J. Biol. Chem. 266*, 9494–9500.
Leatherbarrow, R. J. (1990) *GraFit*, Version 2.0, Erithacus Software Ltd., Staines, U.K.
Lin, T. Y., & Kim, S. P. (1989) *Biochemistry 28*, 5282–5287.
Lu, X., Gilbert, H. F., & Harper, J. W. (1992) *Biochemistry 31*, 4205–4210.
Lyles, M. M., & Gilbert, H. F. (1991) *Biochemistry 30*, 613–619.
Milburn, P. J., Konishi, Y., Meinwald, Y. C., & Scheraga, H. A. (1987) *J. Am. Chem. Soc. 109*, 4486–4496.
Milburn, P. J., Meinwald, Y. C., Takahashi, S., Ooi, T., & Scheraga, H. A. (1988) *Int. J. Pept. Protein Res. 31*, 311–321.
Moroder, L., Gemeiner, M., Göhring, W., Jaeger, E., Thamm, P., & Wünsch, E. (1981) *Biopolymers 20*, 17–37.
Moroder, L., Hübener, G., Göhring-Romani, S., Göhring, W., Musiol, H.-J., & Wünsch, E. (1990) *Tetrahedron 46*, 3305–3314.
Mukaiyama, T., & Takahashi, K. (1968) *Tetrahedron Lett. 56*, 5907–5908.
Nilsson, O., Tapia, O., & van Gunsteren, W. F. (1990) *Biochem. Biophys. Res. Commun. 171*, 581–588.
O'Donnell, M. E., & Williams, C. H. (1983) *J. Biol. Chem. 258*, 13795–13805.
Ravi, A., & Balaram, P. (1983) *Biochim. Biophys. Acta 745*, 301–309.
Ravi, A., & Balaram, P. (1984) *Tetrahedron 40*, 2577–2583.
Rost, J., & Rapoport, S. (1964) *Nature (London) 201*, 185.
Russel, M., & Model, P. (1986) *J. Biol. Chem. 261*, 14997–15005.
Salamon, Z., Gleason, F. K., & Tollin, G. (1992) *Arch. Biochem. Biophys. 299*, 193–198.
Sandberg, V. A., Kren, B., Fuchs, J. A., & Woodward, C. (1991) *Biochemistry 30*, 5475–5484.
Sodano, P., Xia, T.-H., Bushweller, J. H., Björnberg, O., Holmgren, A., Billeter, M., & Wüthrich, K. (1991) *J. Mol. Biol. 221*, 1311–1324.
Söderberg, B.-O., Sjöberg, B.-M., Sonnerstam, U., & Brändén, C.-I. (1978) *Proc. Natl. Acad. Sci. U.S.A. 75*, 5827–5830.
Venkatachalapathi, Y. V., Ventakaram Prasad, B. V., & Balaram, P. (1982) *Biochemistry 21*, 5502–5509.
Weston, J. R., & Schwarz, H. A. (1972) Chemical Kinetics, in *Fundamental Topics in Physical Chemistry* (Johnston, H. S., Ed.) Chapter 1.5, p 11, Prentice-Hall, Englewood Cliffs, NJ.
Wünsch, E., Moroder, L., Göhring-Romani, S., Musiol, H. J., Göhring, W., & Bovermann, G. (1988) *Int. J. Pept. Protein Res. 32*, 368–383.
Xia, T.-H., Bushweller, J. H., Sodano, P., Billeter, M., Björnberg, O., Holmgren, A., & Wüthrich, K. (1992) *Protein Sci. 1*, 310–321.
Zhang, R., & Snyder, G. H. (1989) *J. Biol. Chem. 264*, 18472–18478.